ADVANCED BIOSYSTEMS
www.adv-biosys.com

Collagen Microfibers Induce Blood Capillary Orientation and Open Vascular Lumen

*Hao Liu, Shiro Kitano, Shinji Irie, Riccardo Levato, and Michiya Matsusaki**

Achieving vascularization of engineered tissues or structures is a major challenge in the field of tissue engineering. Hitherto, studies on vascularization have demonstrated limited control of vascular network geometry, such as vasculature direction and network density. An open vascular lumen is crucial to ensure that cells survive and that metabolic activity is fully functional in large-sized tissues. Herein, a method based on high water-dispersible collagen microfibers (CMF) to fabricate capillary orientation-controllable 3D tissue with an open vascular lumen using a dispensing machine is reported. A twenty micrometers-long CMF (CMF-20) with high dispersion property are shown to be more effective for dispensing a homogenous tissue and inducing formation of an interconnected capillary network than two hundred micrometers-long CMF (CMF-200). One of the advantages is the prevention of shrinkage on the *z*-axis of hydrogel-based tissue which acts as a microscaffold. The gaps between the fibers can support endothelial cell migration and maturation, thus forming a larger vascular lumen compared to CMF-free controls. Besides, shear forces produced by the dispensing process cause the collagen microfibers to align, and these microfibers guide cell alignment by integrin-induced adhesion. The findings based on CMF to allow blood capillary alignment and vascular lumen stabilization will be an important technology in tissue engineering.

1. Introduction

The ability to construct 3D tissues with a functionalized capillary network for tissue engineering remains a daunting challenge. Constructing large-scale tissue constructs require an interconnected vasculature to supply the cells inside the 3D tissues with oxygen and nutrients.[1] Lacking a perfusable blood capillary networks with open vascular lumen, tissue structures are limited to several hundred micrometers in thickness.[2] This limitation is due to the insufficient formation of a capillary network to maintain the cell metabolic activity and function. Homogenous capillary networks with a vascular lumen are also required as a functionalized vasculature in full-sized, clinically relevant 3D tissues.[3]

The unique opportunities offered by recent advances in 3D printing can help to build complex 3D structures and these techniques have been adapted to accommodate cells in a process known as bioprinting.[4] Bioprinting provides researchers with control over the spatial positioning of biomaterials and cells, and specifically holds promise for the fabrication of large complex structures with vasculature.[5] Recent efforts to fabricate vascularized tissues via multimaterial bioprinting or stereolithography have been reported.[6–8] However, while these tissues replicate vessels with diameter in the millimeter to hundreds of micrometer-scale, they lack the requisite capillary network and vasculature control (orientation and open lumen) needed to achieve the functionality of designed tissues for future applications. In our body, anisotropic vasculature showing precise directionality can be seen around skeletal and smooth muscles.[9] As an example, myocardial cells are oriented differently for each layer in order to produce sufficient contractile force to supply blood to the whole body.[10] This suggests that the construction of a well-designed parallel blood capillary for each layer of myocardial cells is essential to maintain cell metabolism and function. Therefore, vasculature orientation is important to fabricate a tissue-specific structure artificially.

Collagen is the main structural protein of the extracellular matrix (ECM) and represents 30% of all protein in the human body.[11] Due to its capacity for self-assembly into a fibrillar gel, its amenability for chemical modifications, its low-antigenicity and good biological activity, type I collagen (Col I) is highly suitable as a 3D scaffold material for tissue engineering.[12] In vivo, vascularization is regulated by factors like vascular endothelial growth factor (VEGF),[13] but also by the ECM which enables endothelial cells to adhere and

H. Liu, Prof. M. Matsusaki
Department of Applied Chemistry
Graduate School of Engineering
Osaka University
2-1 Yamadaoka, Suita, Osaka 565-0871, Japan
E-mail: m-matsus@chem.eng.osaka-u.ac.jp

Dr. S. Kitano, Dr. S. Irie
Joint Research Laboratory (TOPPAN) for Advanced Cell Regulatory Chemistry
Graduate School of Engineering
Osaka University
2-1 Yamadaoka, Suita, Osaka 565-0871, Japan

Dr. R. Levato
Regenerative Medicine Center Utrecht and Department of Orthopaedics
University Medical Center Utrecht
Heidelberglaan 100, Utrecht 3584 CX, The Netherlands

The ORCID identification number(s) for the author(s) of this article can be found under https://doi.org/10.1002/adbi.202000038.

DOI: 10.1002/adbi.202000038

proliferate, especially via fibrillar components like Col I,[14] which supports the chemotactic migration of endothelial cells and stimulate vascular tubular morphogenesis.[15] Besides, Col I affect cellular behavior due to its fibrous structure, and directed movement of cells along the fibers or orientated microvascular formation have been achieved based on Col I fiber alignment.[16,17]

In this study, we developed collagen microfibers (CMF) to construct 3D tissues laden with capillary displaying network orientation and with an open vascular lumen, by means of dispensing process. The CMFs we used here have been adapted to fabricate a 3D adipose tissue model, with similar collagen density to the one observed in vivo.[18] The 3D tissues with a homogeneous blood capillary network can be obtained using 20 µm sized CMF in diameter (CMF-20), which can maintain the thickness of the 3D tissues acting also as microscaffolds that induce open vascular lumen stabilization. Moreover, we demonstrated that the integrin interaction between CMF and endothelial cells allows us to fabricate an orientation-controllable capillary network in 3D tissues, when the CMF-20 directionality is guided by shear forces experience during the dispensing process. CMF would be powerful microscaffolds to control blood capillary function in tissue engineering.

2. Results and Discussion

2.1. CMF Fabrication and Characterization

CMF with different sizes were fabricated from Col I sponges after homogenization or sonication (**Figure 1**a). We first confirmed the conformation of the Col I molecule in CMF after homogenization (Figure 1b) by Circular dichroic (CD) spectroscopy. A positive peak at ≈220 nm indicated the typical triple superhelical structure of collagen molecules, which did not appeared in gelatin controls. The CMF and Col I were analyzed by Coomassie Brilliant Blue staining of the 4–20% gradient sodium dodecyl sulfate–polyacrylamide gel electrophoresis (SDS-PAGE) (Figure 1c) and showed the typical pattern for Col I chains with bands at apparent molecular weights of β (215 kDa), $\alpha 1$ (130 kDa), and $\alpha 2$ (115 kDa) in the CMF. These results show that the CMFs after the homogenization retain their triple helix structure and molecular weight of natural Col I. For a more detailed understanding of CMF size after further sonication, the mean fiber length was measured from the phase-contrast (Ph) images (Figure 1d). CMFs after 6 min homogenization were 212 ± 72 µm long with a diameter of 27 ± 8 µm. These values decreased to 26 ± 6 µm in length with a diameter of 4.2 ± 1.8 µm after 100 cycles of sonication

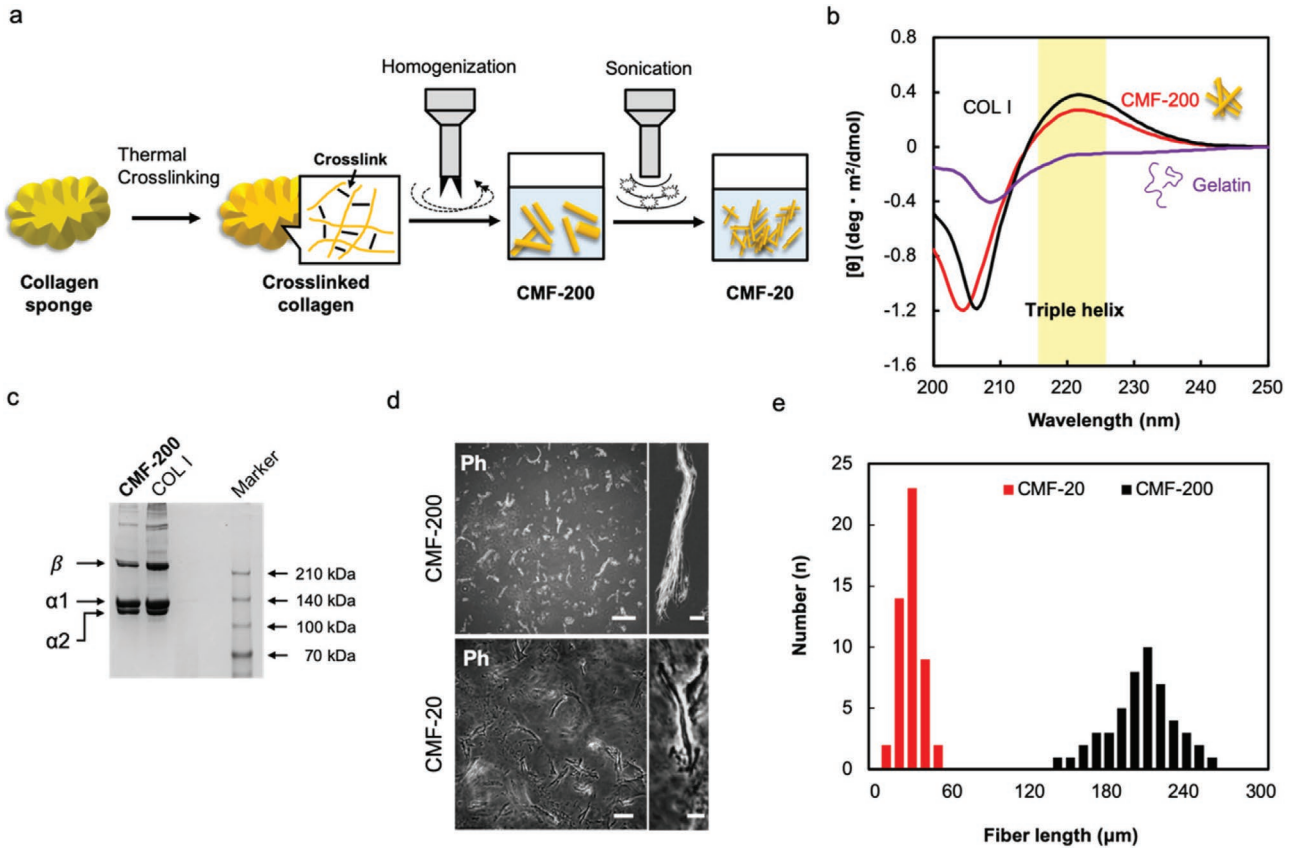

Figure 1. Fabrication and characterization of collagen microfibers (CMF). a) Schematic illustration of CMF-200 and CMF-20 fabricated from the collagen type I sponges. b) Circular dichroism (CD) spectra of 50 µg mL^{-1} CMF-200, collagen type I, and gelatin in 50 × 10^{-3} M acetic acid solution. c) SDS-PAGE analysis of CMF-200 and collagen type I. d) Phase-contrast images of CMF-200 and CMF-20. Right images are magnified images of left. Scale bars are 200 and 20 µm (top) and 20 and 5 µm (bottom). e) Fiber length distribution of CMF-200 and CMF-20 calculated from Ph images in (d) ($n = 50$).

(Figure 1e). We named these two types of CMF as CMF-200 (by homogenization alone) and CMF-20 (by further sonication) according to their length.

2.2. 3D Tissues Fabrication and Capillary Network Formation

Fibrinogen is a protein extracted from the blood, and a fibrin (FB) gel is formed when fibrinogen is mixed with thrombin. FB gel has long been used as a hydrogel matrix to support angiogenesis. Related works have indicated that FB promotes cell adhesion[19] and the synthesis of key ECMs components of basement membrane, which is critical for achieving mature capillary network and vascular lumen formation.[20,21] On the other hand, to maintain the tissue structure and prevent tissue shrinkage caused by collagen during culture, FB gel is often used to increase tissue stability as a secondary cross-link network.[22,23]

Gellan gum (GG) is a water-soluble polysaccharide with thermoreversible gelation property. GG gel is strongly cross-linked by multivalent cations, such as calcium ions.[24] Due to its shear-thinning properties. GG has a relatively low viscosity under shear stress, which makes this material suitable for bioprinting.[25] Recently, we reported a method to construct perfusable endothelialized tunnel structures based on GG gel.[26] GG gels could be completely dissolved in the tris(hydroxymethyl) aminomethane (Tris) buffer, with no detection of cytotoxicity during this process, thus indicating that GG gel have the potential to print capillary tissue with perfusable vasculature.

Therefore, the FB gels and GG gels were selected as hydrogels to embed CMF and endothelial cell, to fabricate the 3D capillary tissues (**Figure 2**a). First, simple droplet-like tissues were prepared using a dispensing machine (Figure 2b). The gelation of 3D tissues using GG gel or FB gel was confirmed after 30 min incubation at 37 °C. The 3D tissues prepared using GG gel displayed a significant shrinkage compared to the fibrin tissue after 7 days of culture. This difference was attributed to the limited ability of cells to adhere onto the pristine GG backbone,[27] which resulted in cells to interact and exert tension forces prevalently with the collagen fiber, shrinking and condensing them within the gel droplet. In contrast, we observed an interconnected blood capillary network formation in the tissues fabricated from FB gel (Figure 2b; Video S1, Supporting Information). FB gel was selected for the subsequent study, due to its ability to support the formation of a homogeneous blood capillary network. For a more detailed understanding of tissue structure stability using FB gel and the confirmation of capillary network formation throughout the culture time, capillary formation at days 5, 7, and 14 were measured from 2D projection images (Figure 2c,d). As shown in the results, the capillary network area is increased from 33% to 58% after 2 weeks of culture. The increase in the mean vascular lumen diameter from 19 to 25 µm further indicated the maturation of the capillary network in these 3D tissues. These results demonstrated that

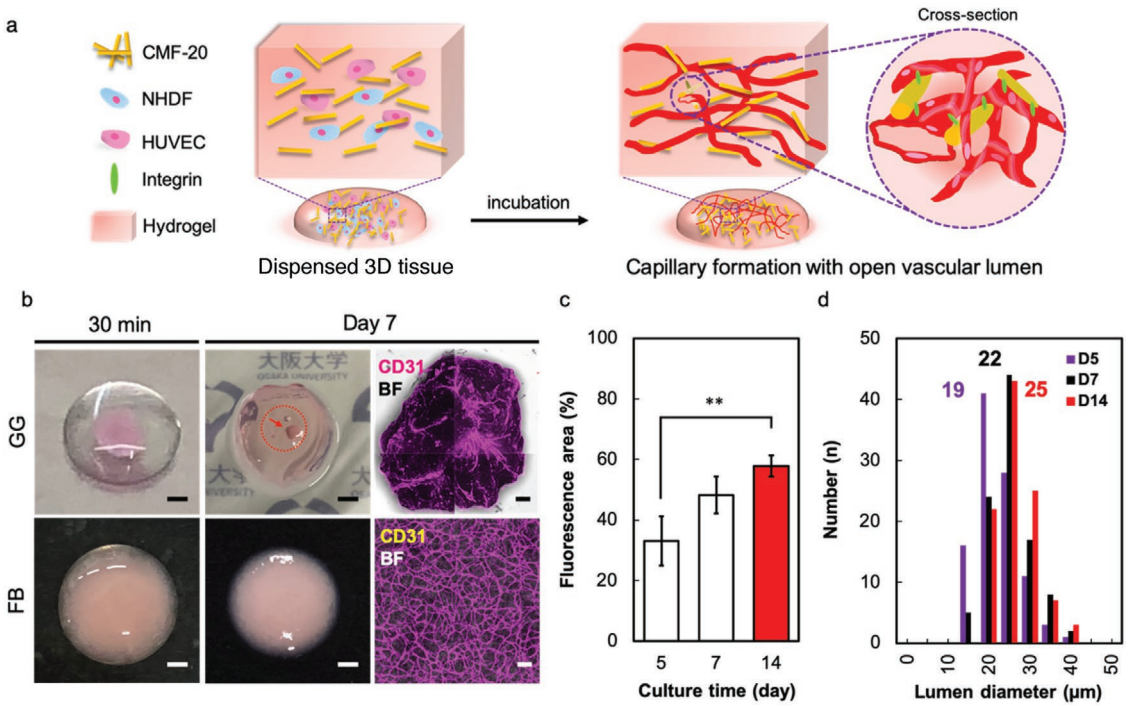

Figure 2. Dispensing of 3D capillary tissue with open vascular lumen. a) Schematic illustration of 3D capillary tissues fabricated by dispensing machine using CMF-20. b) Photographs and confocal laser scanning microscopic (CLSM) images of HUVEC in gellan gum (GG) gel or fibrin (FB) gel 3D tissues after 30 min gelation and subsequent 7 days culture. Scale bars in photographs and fluorescent images are 1 mm and 100 µm respectively. c) Fluorescence area of blood capillary in 3D tissues based on FB gel, stained by anti-CD31 antibody after different culture times ($n = 3$, $^{**}p < 0.01$). d) Distribution of blood capillary lumen diameter after 5, 7, and 14 days culture measured by the anti-CD31 immunofluorescence staining images ($n = 100$). The numbers in (d) indicated the mean vascular lumen diameter.

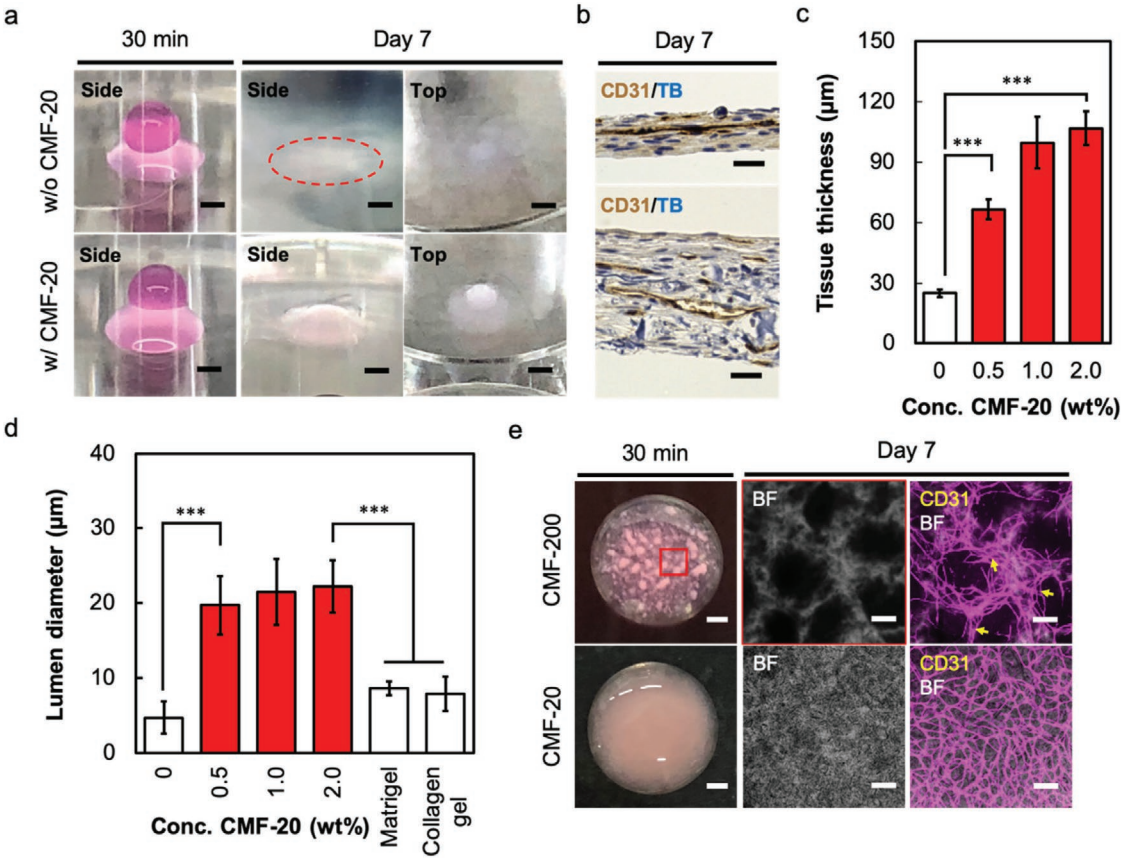

Figure 3. Effect of CMF on the 3D capillary tissues. a) Photographs of two- layered tissue structures with or without CMF-20 after 30 min gelation of the second layer and 7 days culture. Scale bars are 2 mm in all images. b) Histological images stained by anti-CD31 antibody and toluidine blue (TB) of 3D capillary tissues with or without CMF-20 after 7 days culture. Scale bars are 20 μm. c) The mean tissue thickness of 3D capillary tissues at different CMF-20 concentrations measured from histological images ($n = 3$, over 20 per sample). d) The mean capillary lumen diameters of 3D capillary tissues at different CMF-20 concentrations compared to the Matrigel and 0.1 wt% collagen type I gel measured from histological images ($n = 3$, over 40 areas per sample, $^{***}p < 0.001$). e) Photographs and CLSM images of 3D capillary tissues stained with anti-CD31 antibody using CMF-200 and CMF-20 after 30 min gelation and 7 days culture. Scale bars are 1 mm and 200 μm, respectively. Yellow arrows indicate blood capillary close to the aggregated CMF-200.

3D capillary tissue using FB gel can prevent tissue shrinkage and induce a self-organized capillary network formation.

2.3. Capillary Lumen in 3D Tissues and CMF Size Effect

To demonstrate the vital role of CMF in maintaining the 3D tissue structure, we dispensed a second layer on the top of the first layer gels to fabricate a double-layer structure using FB gel. Since sufficient mechanical strength is required to maintain the double-layer structure, the dispensing of the second layer began after the gelation of the bottom layer. After 30 min gelation of the second layer, we confirmed both tissues with or without CMF-20 had a double-layer structure (**Figure 3**a). However, the control group without CMF-20 showed a significant shrinkage in the *z*-direction after 7 days of culture because in absence of the CMF fibers, the cell induced shrinkage of FB gel. The shrinkage phenomena may not be suitable for tissue engineering, in order to preserve the shape-fidelity of the tissue construct. In contrast, a double-layer structure with a 0.5 wt% of CMF-20 was found to retain the visible double-layer structure at *z*-direction. The shrinkage percentage in the double-layer tissue decreased from 83% (w/o CMF-20) to 70% (w/ CMF-20). We compared the tissue thickness with different CMF-20 concentrations from 0 to 2 wt% after 7 days of culture. More than two-fold increment in tissue thickness between CMF-free controls and a 0.5 wt% CMF-20 were found after 7 days, even there is no significant difference in thickness just after tissue preparation (Figure 3b,c; Figure S2a, Supporting Information). These differences in thickness shown that increasing CMF-20 concentration can effectively reduce the shrinkage of the tissues and maintain its 3D structure.

Interestingly, in tissues without CMF-20, we measured that the average diameter of vascular lumen was 4 μm from histological cross-section images (Figure 3d). In contrast, in the 3D tissues with a CMF-20 concentration of 0.5% or more, the diameters of the vascular lumen were greater than 20 μm (Figure 3d; Video S2, Supporting Information). To further demonstrate this difference, we measured the formation of the vascular lumen in commercially available gels under the same conditions.

Even though commercially available collagen gels or Matrigel can support the formation of interconnected capillary networks (Figure S2b, Supporting Information), most vascular lumens have an inner diameter of less than 10 μm. However, in the 3D capillary tissue fabricated from a mixture of Matrigel and CMF-20, an increase in open vascular lumen was found in histological cross-section images (Figure S2c, Supporting Information). Accordingly, we hypothesized that the embedded CMF-20 act as a microscaffold that could provide spaces for migration of endothelial cells, and support capillary maturation to form an open vascular lumen.

To explain further, the spaces between microfibers have a significant impact on vascular lumen in the 3D tissues. We fabricated different 3D tissues with CMF-20 concentration from 1 to 20 wt%. The distances between the microfibers was measured from the histological analysis (H&E staining) and the mean size of these gaps was ascertained. As the concentration of CMF-20 increased from 1 to 20 wt%, the distances decreased from 32 ± 15 to 11 ± 4 μm (Figure S3a,c, Supporting Information). On the other hand, we measured the size of the vascular lumen in 3D tissues with different spacings (Figure S3b,d, Supporting Information). To eliminate differences in maturity between different stages of vascularization, we cultured all tissues for two weeks. Interestingly, the mean space between fibers was about 32 μm when tissue with 1 wt% of CMF-20, the vascular lumen diameters were mainly distributed at 9 and 28 μm (Figure S3b,d, Supporting Information). As shown in the immunohistological images, these correspond to two different blood vascular structures, true capillary (blue arrows) and venule (red arrows). However, when the CMF-20 concentration increased to 20 wt%, the vascular lumen diameter was mainly distributed at about 9 μm. This finding indicates that the vascular diameter could be adjusted by controlling the size of the spaces between the fibers. In other words, we can control the size of the spaces between the fiber structures in different tissues regions by changing the concentration of CMF-20, and customize different vascular structures in different areas of large-sized 3D tissue. These results demonstrate the potential for the fabrication of complex vascular trees using CMF-20.

Next, we investigated the effect of CMF sizes on capillary formation, 3D tissues fabricated from CMF-200 and CMF-20 were examined to understand the differences in tissue structure and vascularization (Figure 3e). We found that the dispensing process was unstable using CMF-200 (Figure S7, Supporting Information), and a significant aggregation of CMF-200 had appeared in the 3D tissues. The aggregation of CMF-200 could not be improved even after 7 days of culture, and this also lead to a less capillary formation and no interconnection. In contrast, the capillary tissue using size reduced CMF-20 showed homogeneity in both the tissue structure and the formation of an interconnected capillary network (Figure 3e). This indicated that the CMF-20 with a smaller size could be used to fabricate 3D tissues with a homogeneous capillary network.

The aforementioned findings demonstrate the advantages of CMF-20 as a microscaffold as it maintains a homogenous 3D tissue structure and allows for the customization of different vascular structure formations by control of the spaces size.

2.4. Dispensing and Control of Capillary Orientation

To further build onto these results, we fabricated capillary structures with flexible shapes based on CMF-20 and FB gel to understand dispensing resolution (**Figure 4**a,b). For example, a star-like 3D tissue (Figure 4a), or a series of droplets with different diameters from 5.7 to 1.7 μm were fabricated. Even after automated dispensing, homogeneous blood capillary networks were formed using CMF-20. Moreover, cells in 3D tissue could maintain high cell viability (Figure S3, Supporting Information) at CMF-20 concentration from 0 to 2 wt%. We measured the capillary formation in droplets tissues from the immunofluorescence images (CD31). Although smallest fabricated tissue diameter in 1.7 mm, the capillary networks were clearly found in the whole tissue structure with 16% density over tissue area (Figure 4b).

Moreover, we also found an interesting phenomena, as the endothelial cells orientated themselves preferentially in the same direction of the CMFs, even when aggregated CMF-200 were used. Although the blood capillary formation was not homogenous, the endothelial cell stills made full use of the extracellular matrix as scaffolds, and the capillary distributed along the surface or spaces of CMF-200 (Figure 3e, yellow arrows). To further investigate the effects of the fiber structure of CMF-20 on angiogenesis orientation and the interaction between CMF and endothelial cells, we prepared a series of line tissues with different CMF-20 concentrations from 0 to 2 wt% (Figure 4c). Promisingly, after 7 days of culture, the capillary network formed in the tissue was highly overlapping with the directionality of the oriented CMF-20 orientation. To quantitatively evaluate the distribution of blood capillary orientation and to understand the effect of CMF-20 on the capillary orientation, we defined a coordinate system in the line tissue. The orientation was set to 0° and the capillary orientation segment angles were measured using ImageJ. The range of angles from 10° to –10° was selected as the target directionality in the capillary orientation segment angle distribution (Figure 4d). The percentage of orientated capillaries within the target angle slightly increased with increasing CMF-20 concentration. It increased from 38% to 53% at CMF-20 concentration of 0 and 2 wt%, respectively, showing a significant difference (Figure S5, Supporting Information). Immunofluorescence analyses of Col I indicated a large amount of collagen molecules in the periphery of the blood capillaries, suggesting the relationship between CMF-20 and blood capillary.

For further confirmation of the possibility of capillary orientation control and to understand the interaction between endothelial cells and CMF-20, we performed integrin β1 expression in the 3D tissue with or without CMF-20 (Figure 4e). Integrin β1 expression was found to be greater in the tissues with CMF-20 and located close to the capillaries in 3D tissues. Furthermore, we also found the integrin β1 expression surrounding the blood capillary with lumen structure from cross-section images, but not in the tissues without any CMF-20 (Figure 4e, right). The results also showed that endothelial cells adhered to the surrounding CMF-20 by integrin, and matured to form a vascular lumen. When the CMF-20 in the bioink is dispensed, it can be aligned in the dispensing direction due to its high viscosity under the shearing force (Figure S6, Supporting Information).

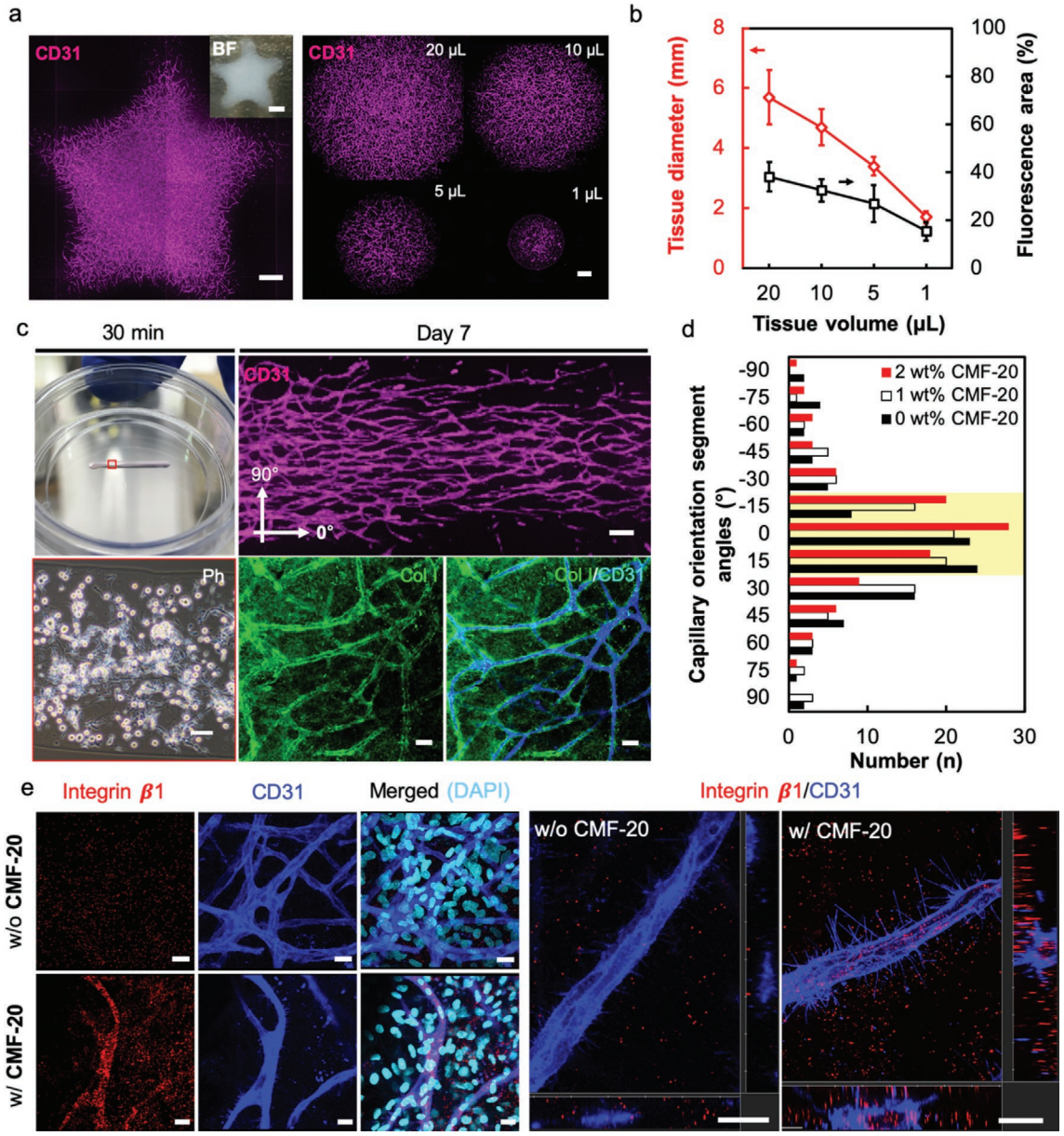

Figure 4. Control of blood capillary alignment in the 3D capillary tissues using CMF-20. a) Fluorescence images of 3D capillary tissues with star-like shape (left) and with different tissue volumes (right). Inserted image is a photograph of the star-like shaped tissue. Scale bars at left are 1 and 3 mm in insertion and at right is 500 μm. b) The average fluorescence area and mean tissue size with different dispensing volumes ($n = 3$). c) Photograph (top left), phase contrast image (bottom left), and CLSM images stained anti-CD31 antibody (top right) of the line 3D capillary tissues after 30 min gelation and 7 days culture. CLSM images of CMF-20 and blood capillary stained with anti-col I and CD31 antibodies after 7 days culture (bottom, right). Scale bars are 200 μm in Ph and top right fluorescence image, 50 μm in bottom right fluorescence images. d) Orientation angle distribution of blood capillary in 3D capillary tissues at different CMF-20 concentrations ($N = 100$) measured from CLSM images in c) top right. e) The CLSM images of blood capillary and integrin $\beta 1$ stained by anti-CD31 and integrin antibodies. Reconstructed 3D-CLSM cross-section image of the tissues stained by anti-CD31 and integrin antibodies. Scale bars are 20 μm.

The CMF-20 alignment helps endothelial cell adhesion through integrin molecules, and integrin interactions induce capillary alignment and vascular lumen formation.[28,29] Overall, these results provide a novel, fundamental technology to enable the control of directionality over endothelial cell self-assembly into capillary networks, thus permitting to guide the architecture of microvascular structures. This technology shows promising applications for the formation of tissue engineered constructs.

3. Conclusion

The fabricated CMF maintained similar triple helix structure and molecular weight of natural Col I after thermal cross-linking and processing to break the microfibers into smaller fragments. The lower fiber size (CMF-20) showed a higher water dispersibility and interconnected capillary network than the lager fiber size (CMF-200), and a homogeneous tissue

structure can effectively induce self-organized vascularization. The results from the vascular and 3D tissue structures indicated that CMF-20 is essential for maintaining tissue structure by acting as a microscaffold. The open vascular lumen with a larger diameter ensures that obtained capillary networks can be used to efficiently deliver oxygen and nutrients to core areas of the 3D tissue. Additionally, the orientation behavior of CMF-20 caused by the shearing force during dispensing process can yield a complex tissue with aligned collagen microfibers. These oriented microscaffolds have also been shown to achieve an oriented capillary network, potentially through the interaction between integrins and CMF-20. This method can be used to control capillary orientation in 3D tissues with highly oriented vasculature, such as muscle tissue. Tailored capillary tissues based on CMF-20 are expected to be combined with a variety of cells to fabricate fully functional tissues with a complex vasculature in the future.

4. Experimental Section

Materials: Collagen Type 1 sponges were kindly provided by Nippon ham (Osaka, Japan) and GG (M_w = 500 kDa) was obtained from Sansho (Osaka, Japan). Fibrinogen (from bovine plasma, F8630), thrombin (from bovine plasma, T4648), bovine serum albumin (BSA, A3294), phosphate buffered saline powder (PBS, D5652), and Triton-X 100 (T8787) were purchased from Sigma-Aldrich (MO, USA). Fetal bovine serum (35010CV) and Matrigel were purchased from Corning (NY, USA). Goat anti-mouse secondary antibody (Alexa Fluor 647, A21235), Hoechst 33 324 (H3570) and Qubit dsDNA Assay kit (High-sensitive, Q32851) were obtained from Thermo Fisher Scientific (MA, USA). 4%-paraformaldehyde (PFA, Wako, 16 310 245), Goat anti-rabbit secondary antibody (Alexa Fluor 488, Abcam, ab150077), Monoclonal mouse anti-human CD31 antibody (Wako, M0823), Anti-integrin beta 1 antibody (Abcam, ab134179), Anti-collagen type 1 antibody (Abcam, ab34710) were used without further purification. Normal human dermal fibroblast (NHDF, CC2509), human umbilical vein endothelial cell (HUVEC: C25271) were cultured in Dulbecco modified Eagles's medium (DMEM High-Glucose, Nacalai tesque, 0 8458) with antibiotics (Nacalai tesque, 0 2894) and endothelial growth medium (EGM-2MV, Lonza, CC4147) respectively.

Preparation of Collagen Type I Microfibers and 3D Capillary Tissue: Based on a previous study, the CMF-200 was fabricated from a collagen type I sponge after dehydration condensation at 200 °C for 24 h cross-linking.[30] The cross-linked collagen sponge was mixed with 10× PBS solution at a concentration of 10 mg mL^{-1} (pH = 7.4, 25 °C) and homogenized for 6 min at 30 000 rpm (Violamo VH-10 homogenizer, S10N-10G with 10 mm diameter and 115 mm length probe). The CMF-20 suspension was obtained under further ultrasonication (Ultrasonic processor VC50, 50 W, 20 kHz) in an ice bath for 100 cycles (1 cycle comprised 20 s ultrasonication and 10 s cooling). The solution was transferred in a glass recipient after filtration (40 µm filter, microsyringe 25 mm filter holder, Merck), then the filtrate was freeze-dried for 48 h (Freeze dryer FDU-2200, Eyela Co.). The obtained CMF-200 and CMF-20 were kept in a desiccator at room temperature.

Fabrication of 3D Capillary Tissue Manually: NHDF and HUVEC were trypsinized (5 min, 37 °C) and collected by centrifugation (5 min, 1000 rpm, room temperature). The supernatant was removed before dispensing. 3 mg CMF-20 was mixed with 3 U thrombin in 100 µL DMEM. Then, 2 mg Fibrinogen was mixed with 1×10^6 NHDF and 5×10^5 HUVEC in 200 µL DMEM (FBS free). 3D capillary tissue using Matrigel or Col I gel was prepared following the commercial protocol. Briefly, Matrigel solution was mixed with CMF-20 and cells at 4 °C, and 3D tissues were obtained after 30 min incubation at 37 °C. Col I gel was prepared from collagen solution and NaOH was mixed with gentle pipetting. The pH was confirmed with a pH strip. The successfully prepared collagen solution had a pH of around 7.4. It was then kept on ice and mixed with CMF-20 and cells. The mixture was stored at 37 °C, in atmospheric humidity to fabricated collagen gel.

Fabrication of 3D Capillary Tissue by Dispensing: 3 mg of CMF-200 or CMF-20 was mixed with 3 U thrombin in 100 µL DMEM. Then, 2 mg of Fibrinogen was mixed with 1×10^6 NHDF and 5×10^5 HUVEC in 200 µL DMEM (FBS free). The solutions were transferred to a glass syringe (1 mL Gastight Syringe Model 1001 TLL, 81 320, Hamilton) with standard metal needles (SNA 19 G& 21 G, Musashi Engineering, Inc.). The syringe was set on a dispenser (NANO MASTER SMP-III, Musashi Engineering, Inc.) using an adapter and keep the dispensing system at room temperature. Two dispenser moving speeds (2 and 4 mm s^{-1}) and three different dispensing speeds (0.04, 0.08, and 0.16 mm s^{-1}) were selected, and dispensing parameters were optimized to obtain 3D tissues with a high-quality structure. The dispensing programs were designed on MuCADV (Software for editing the dispensing pattern, Musashi Engineering, Inc.) and completed debugging before dispensing. The line tissues with the oriented capillary network were fabricated using 21 G needle with a 2 mm s^{-1} of dispenser moving speed and 0.04 mm s^{-1} dispensing speed. 3D tissues were stored at 37 °C 30 min to ensure gelation prior to the addition of mixed medium (1:1 DMEM and EGM-2MV). 3D tissues were incubated for 7 days at 37 °C, 5% CO_2, with medium changes every 2 days.

Fluorescence Imaging and Histological Analysis: The nuclei were stained with Hoechst and HUVEC were detected by the anti-CD31 antibody. Briefly, the tissues were fixed in 4% paraformaldehyde (30 min, room temperature) and permeabilized with 0.02% Triton X-100 (15 min). The tissues were blocked with 1 wt% BSA (1× PBS, pH 7.4, 2 h) and then incubated with the primary antibodies (anti-CD31 antibody, anti-collagen type 1 antibody and anti-integrin beta 1 antibody, diluted at 1/50 in BSA) for at least 12 h. After washing the tissues with 1× PBS, the secondary antibodies (goat-anti mouse, Alexa Fluor 647; goat-anti rabbit, Alexa Fluor 488, 1:200 dilution in BSA) were added. After a PBS rinsing cycle, the 3D tissue was finally observed using a confocal laser scanning microscope (Confocal Quantitative Image Cytometer CQ1, Yokogawa, Japan; CLSM Fluoview FV3000, Olympus, Japan and CLSM, Fluoview FV10i, Olympus, Japan). For histology staining, the fixed 3D tissues were rinsed three times in PBS and sent to the Applied Research Company for paraffin embedding. Sectioned 3D tissues were stained with hematoxylin eosin (HE) or CD31 (Abcam, ab182981) staining. The images were captured using an FL EVOS Auto microscope (Thermo Fisher). Analysis of the fluorescence and histological images were conducted using ImageJ Fiji software for 3D tissue thickness, fluorescence area, capillary lumen diameter and length calculation. Images of the 3D reconstructed capillary and surface were obtained using Imaris software (ver. 9.2.1, Oxford Instruments).

Rheological Characterization of the Prepared Bioink: The rheological properties of prepared bioinks with different CMF-20 concentrations were assessed using an HAAKE Rheo Stress 6000 rheometer (Thermo Fisher Scientific). Temperature was maintained at 25 °C during testing. The blended bioinks were prepared as mentioned above immediately prior to the rheological measurements and then loaded into the gap between the parallel upper and lower plates of the rheometer. Viscosity was measured at a constant frequency (1 Hz) during a shear rate sweep of 10–1000 s^{-1} within 10 min using a 35 mm, 1° cone plate geometry (C35/1).

Toxicity Assays: After 30 min gelation and 24 h culture, the cell viability was checked using Live/Dead Staining (Molecular Probes, Thermo Fisher Scientific) without further purification. After rinsing three times with PBS, the 3D tissues were exposed to 1/500 diluted Ethyl Bromide (Red, dead cells), 1/125 diluted Calcein (Green, live cells) and 1/1000 diluted Hoechst (1 h, 37 °C). The fluorescence imaging followed the previously described protocol using CQ1. Imaris software was used to analyze the signal colocalization coefficient from 2D projection images.

Statistics: Statistical analysis was performed using a two-tailed Student's *t*-test. The values and error bar represent the means significantly different from three independent experiments. A *p*-value

less than 0.05 was considered to be statistically significant. *N.S.* denotes no significant difference.

Supporting Information

Supporting Information is available from the Wiley Online Library or from the author.

Acknowledgements

The authors acknowledge financial support by Grant-in-Aid for Scientific Research (B) (Grant No. 17H02099) and JST Mirai-Program (Grant No. 18077228).

Conflict of Interest

The authors declare no conflict of interest.

Keywords

blood capillary, capillary orientation, collagen microfibers, vascular lumen

Received: February 1, 2020
Revised: February 15, 2020
Published online: March 12, 2020

[1] J. Rouwkema, A. Khademhosseini, *Trends Biotechnol.* **2016**, *34*, 733.
[2] S. Levenberg, J. Rouwkema, M. Macdonald, E. Garfein, D. Kohane, D. Darland, R. Marini, C. van Blitterswijk, R. Mulligan, P. D'Amore, R. Langer, *Nat. Biotechnol.* **2005**, *23*, 879.
[3] P. Johnson, A. Mikos, J. Fisher, J. Jansen, *Tissue Eng.* **2007**, *13*, 2827.
[4] J. Groll, T. Boland, T. Blunk, J. Burdick, D. Cho, P. Dalton, B. Derby, G. Forgacs, Q. Li, V. Mironov, L. Moroni, M. Nakamura, W. Shu, S. Takeuchi, G. Vozzi, T. Woodfield, T. Xu, J. Yoo, J. Malda, *Biofabrication* **2016**, *8*, 013001.
[5] S. Paulsen, J. Miller, *Dev. Dyn.* **2015**, *244*, 629.
[6] D. Kolesky, K. Homan, M. Skylar-Scott, J. Lewis, *Proc. Natl. Acad. Sci. USA* **2016**, *113*, 3179.
[7] J. Miller, K. Stevens, M. Yang, B. Baker, D. Nguyen, D. Cohen, E. Toro, A. Chen, P. Galie, X. Yu, R. Chaturvedi, S. Bhatia, C. Chen, *Nat. Mater.* **2012**, *11*, 768.
[8] B. Grigoryan, S. Paulsen, D. Corbett, D. Sazer, C. Fortin, A. Zaita, P. Greenfield, N. Calafat, J. Gounley, A. Ta, F. Johansson, A. Randles, J. Rosenkrantz, J. Louis-Rosenberg, P. Galie, K. Stevens, J. Miller, *Science* **2019**, *364*, 458.
[9] R. Lieber, J. Fridén, *Muscle Nerve* **2000**, *23*, 1647.
[10] I. LeGrice, B. Smaill, L. Chai, S. Edgar, J. Gavin, P. Hunter, *Am. J. Physiol.: Heart Circ. Physiol.* **1995**, *269*, H571.
[11] W. Friess, *Eur. J. Pharm. Biopharm.* **1998**, *45*, 113.
[12] E. Antoine, P. Vlachos, M. Rylander, *Tissue Eng., Part B* **2014**, *20*, 683.
[13] E. Ruoslahti, *Nat. Rev. Cancer* **2002**, *2*, 83.
[14] G. Davis, D. Senger, *Circ. Res.* **2005**, *97*, 1093.
[15] E. Dejana, L. Languino, N. Polentarutti, G. Balconi, J. Ryckewaert, M. Larrieu, M. Donati, A. Mantovani, G. Marguerie, *J. Clin. Invest.* **1985**, *75*, 11.
[16] W. Han, S. Chen, W. Yuan, Q. Fan, J. Tian, X. Wang, L. Chen, X. Zhang, W. Wei, R. Liu, J. Qu, Y. Jiao, R. Austin, L. Liu, *Proc. Natl. Acad. Sci. USA* **2016**, *113*, 11208.
[17] M. McCoy, J. Wei, S. Choi, J. Goerger, W. Zipfel, C. Fischbach, *ACS Biomater. Sci. Eng.* **2018**, *4*, 2967.
[18] F. Louis, S. Kitano, J. Mano, M. Matsusaki, *Acta Biomater.* **2019**, *84*, 194.
[19] R. Rao, A. Peterson, J. Ceccarelli, A. Putnam, J. Stegemann, *Angiogenesis* **2012**, *15*, 253.
[20] C. Wong, E. Inman, R. Spaethe, S. Helgerson, *Thromb. Haemostasis* **2003**, *89*, 573.
[21] N. Broguiere, L. Isenmann, C. Hirt, T. Ringel, S. Placzek, E. Cavalli, F. Ringnalda, L. Villiger, R. Züllig, R. Lehmann, G. Rogler, M. Heim, J. Schüler, M. Zenobi-Wong, G. Schwank, *Adv. Mater.* **2018**, *30*, 1801621.
[22] J. Lee, H. Kim, H. Kim, S. Lee, M. Gye, *Biomaterials* **2006**, *27*, 2845.
[23] D. Eyrich, F. Brandl, B. Appel, H. Wiese, G. Maier, M. Wenzel, R. Staudenmaier, A. Goepferich, T. Blunk, *Biomaterials* **2007**, *28*, 55.
[24] E. Miyoshi, *Carbohydr. Polym.* **1996**, *30*, 109.
[25] T. Otsuji, J. Bin, A. Yoshimura, M. Tomura, D. Tateyama, I. Minami, Y. Yoshikawa, K. Aiba, J. Heuser, T. Nishino, K. Hasegawa, N. Nakatsuji, *Stem Cell Rep.* **2014**, *2*, 734.
[26] M. Matsusaki, H. Ikeguchi, C. Kubo, H. Sato, Y. Kuramochi, D. Takagi, *ACS Biomater. Sci. Eng.* **2019**, *5*, 5637.
[27] C. Ferris, K. Gilmore, G. Wallace, M. Panhuis, *Soft Matter* **2013**, *9*, 3705.
[28] J. Humphries, *J. Cell Sci.* **2006**, *119*, 3901.
[29] T. Twardowski, A. Fertala, J. Orgel, J. San Antonio, *Curr. Pharm. Des.* **2007**, *13*, 3608.
[30] S. Gorham, N. Light, A. Diamond, M. Willins, A. Bailey, T. Wess, N. Leslie, *Int. J. Biol. Macromol.* **1992**, *14*, 129.

